Multiple ionization and fragmentation of polyatomic molecules by fast heavy ions

Journal of Physics: Conference Series **288** (2011) 012027 doi:10.1088/1742-6596/288/1/012027

Multiple ionization and fragmentation of polyatomic molecules by fast heavy ions

A. Itoh, T. Mizuno* and T. Majima

Department of Nuclear Engineering, Kyoto University, Kyoto 606-8501, Japan

E-mail: itoh@nucleng.kyoto-u.ac.jp

Abstract. We investigated molecular fragmentation for CO, C_2H_2 and C_{60} molecules induced by impact of various fast heavy ions. Fragment ions produced in electron capture and loss collisions of projectile ions were measured in coincidence with final projectile charge states. As for C_{60}target, the number distribution of secondary electrons emitted in single collision event were also measured by means of a triple coincident method. The charge state distribution of transiently formed C_{60}^{r+} was successfully reproduced by our new model calculation on the basis of statistical energy deposition model developed for polyatomic molecules. Data acquisition using position sensitive detection system allows us to obtain 3D momentum imaging of fragment ions from CO and C_2H_2 molecules. Typical results relevant to molecular orientation effect and kinetic energy release (KER) are discussed.

1. Introduction

Molecular fragmentation by an external force exerted from a charged particle and a photon has been the subject of increasing attention to date [1, 2, 3]. In a collision with an energetic swift ion, a target molecule receives a considerable amount of electronic energy, leading to molecular excitation, fragmentation and multiple ionization as well. Furthermore, the amount of electronic energy deposition into a target is supposed to vary considerably depending on the impact parameter between collision partners and on the orientation of the target molecule. Hence, acquisition of various information about these quantities is important to achieve complete understanding of collision-induced molecular excitation and relaxation mechanisms.

On the other hand, recent and rapid development of multicoincidence and momentum imaging techniques allows one to deduce important parameters such as molecular orientation before collisions, kinetic energy of fragment ions, initial charge state of molecules prior to dissociation, and so forth. Investigation using this technique extends from diatomic to polyatomic molecules including C_{60} and biomolecules [4, 5]. To date, however, collision induced molecular fragmentation using MeV energy heavy ions is not fully understood yet.

In this paper, we investigate fragmentation as well as ionization of diatomic through C_{60} molecules induced by fast heavy ions with velocities higher than the Bohr velocity 2.2×10^8cm/s. In order to gain an insight into collision dynamics in molecular fragmentation, measurements were made under charge-changing conditions where the incident charge state of a projectile particle changes via electron capture/loss collisions with a target particle.

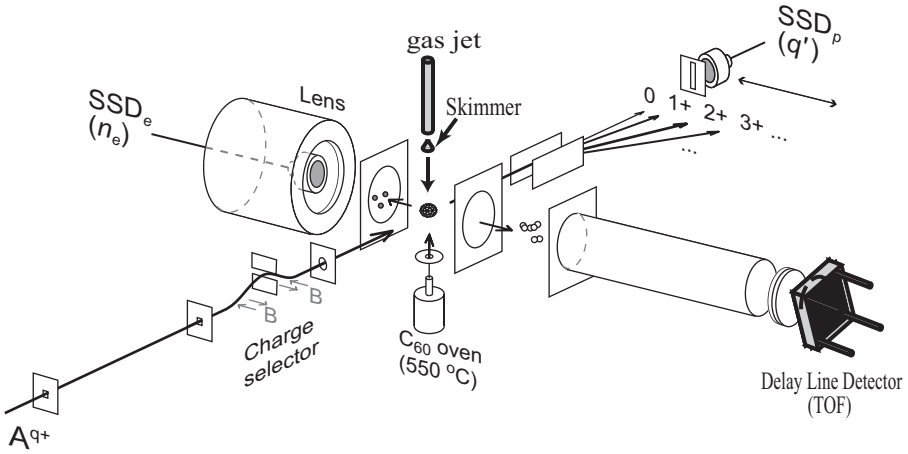

Figure 1. Schematic of experimental setup of the TOF-n_e coincidence measurements.

2. Experimental

Experiments were performed at the QSEC 1.7-MV tandem accelerator facility of Kyoto University. The experimental apparatus and method are described elsewhere [6, 7], and an essential outline is given here. Figure 1 shows a sketch of our experimental setup. A beam of A^{q+} extracted from the accelerator was carefully collimated to about 0.1 mm in diameter and was charge purified with a magnetic charge-selector before entering a collision chamber. Here A stands for a projectile species with a charge state q. After passing through a gaseous jet target the projectile particles were charge separated horizontally by an electrostatic deflector and detected by a movable solid state detector (SSD) which had a rectangular entrance slit of 0.5mm$\times$ 5 mm. The acceptance angle of SSD for scattered particles were about $\pm$0.4 mrad (horizontal) and $\pm$4 mrad (vertical), respectively.

Projectile ions studies in this work are 2.0MeV C^+, 6.0MeV O^{4+}, and 2.0-6.0 MeV $Si^{2+,3+}$ ions. Gaseous molecular jet targets are CO, C_2H_2 and C_{60}. As for a C_{60} target, we produced an effusive molecular beam by sublimation of high-purity powder in a quartz oven heated at 550°C as shown in Fig. 1. The diameter of the C_{60} beam in a collision region was estimated to be smaller than 4 mm. CO and C_2H_2 targets were produced from a nozzle with a skimmer.

Fragment ions were extracted perpendicular both to the incident beam and the molecular beam and were detected by a two-stage multichannel-plate detector. Mass-to-charge of product ions was measured with a time-of-flight (TOF) spectrometer operated under a Wiley-McLaren spatial-focusing condition. Data acquisition was made by using a fast-multichannel scaler (LN-6500,Labo.) for C_{60} experiments and a position-sensitive delay-line detector system (DLD-40, Roentdeck) [8] for other molecules. Both detection systems enable us to detect plural fragment ions produced in a single collision event.

Secondary electrons emitted from C_{60} were also measured with a SSD on which a positive voltage of 30 kV was applied. Hence, the pulse height of signals from this SSD is proportional to a total energy $30n_e$ keV when n_e electrons are detected simultaneously. Hence, a pulse height distribution provides a number distribution of secondary electrons. The position-sensitive DLD system provides initial momentum vectors of plural fragment ions and an information about angular correlation between them can be derived. Measurements were made in coincidence with

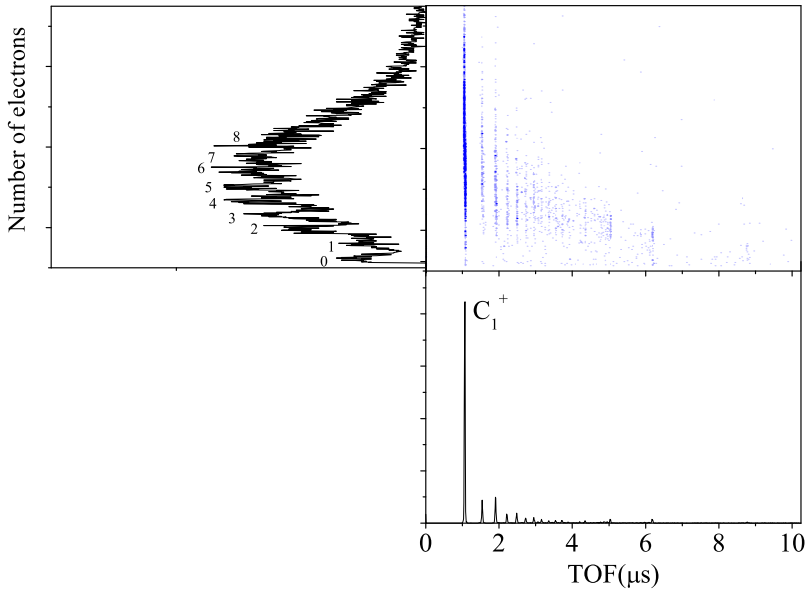

Figure 2. (Color online) Fragment ion spectrum and the number distribution of electrons in 1e-loss collisions of 6.0 MeV Si^{3+} with C_{60}.

charge-selected projectile particles at different scattering angles.

3. Results and discussion

3.1. C_{60} fragmentation

Figure 2 presents a typical example of correlation map between fragment ions (horizontal) and simultaneously emitted secondary electrons (vertical), measured for single electron loss collisions of 6.0 MeV Si^{3+} with C_{60}. It can be seen clearly that C_{60} is completely disintegrated into small-size fragment ions dominated by C^+ and the secondary electron spectrum exhibits a broad Gaussian-type distribution centered at the number of electrons of about 7.

From this map one can derive a series of n_e-distributions correlated with individual fragment ions and vice versa. It is emphasized that one can specify the transiently formed charge states of C_{60}^{r+} as we know the final charge state of projectiles and the total number of ionized electrons in addition to the charge state of fragment ions. We found that the multifragmentation of C_{60} begins at small degree of ionization of $r = 3$ [9]. It turned out that the key quantity charactering the multifragmentation of C_{60} is the internal excitation energy rather than the initial charge state r. The internal energy E_{int} is a part of total energy deposition into a C_{60} molecule E_d which varies significantly at different impact parameters b between collision partners. Figure 3 shows how the fragment ion distribution changes so dramatically when the impact parameter is different [6]. Here, two TOF spectra were obtained at scattering angles of 0 mrad and 0.8 mrad in two-electron loss collisions of 2MeV Si^{2+} with C_{60}. One can see obviously that only small fragment ions, resulting from complete molecular disintegration, are produced at 0.8 mrad, while at 0 mrad intact parent ions C_{60}^{r+} with $r = 1 - 4$ are also produced rather strongly. This completely different spectral feature indicates clearly that the value of E_d in close collisions is undoubtedly much larger than that in distant collisions. Also, we found that

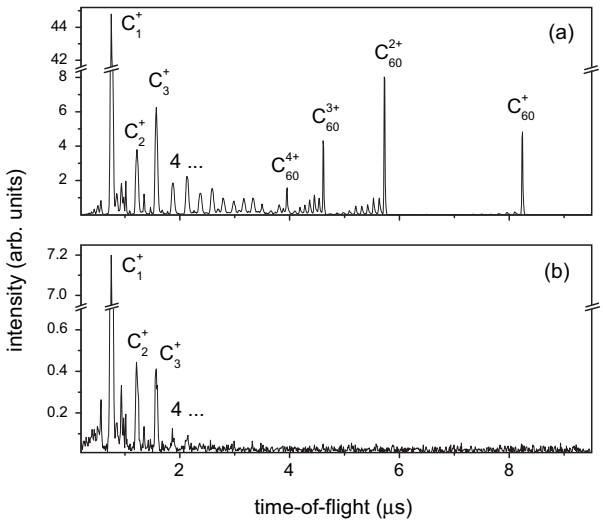

Figure 3. Comparison of TOF spectra for $2e$ loss collisions measured at two scattering angles; (a) $\theta = 0 \pm 0.4$mrad, and (b) $\theta = 0.8 \pm 0.4$mrad. 2.0 MeV Si^{2+} with C_{60}.

the mass distribution changes significantly in electron loss and capture collisions. Qualitatively to say, electron capture can take place in relatively distant collisions and electron loss may be limited to only close collisions because the electron loss is the ionization of a charged projectile ion by a neutral target molecule.

As the geometrical structure of C_{60} is known precisely, the yield of outgoing projectile particles scattered into various angles can be calculated numerically. The scattering yield of 2.0 MeV C^+ into $\theta = 0$, 0.5 and 1.0 mrad are depicted in Fig. 4 as a function of the impact parameter b measured from the C_{60} center [10]. The number density of carbon atoms is depicted in the upper figure. We found that scattering into $\theta \neq 0$ is essentially limited to $b \leq 7$ corresponding to the radius of C_{60}. Together with the data of TOF spectra at different θ, we found that small fragment ions C_m^+ $(m = 1-3)$ are produced in cage-penetration collisions and intact parent ions C_{60}^{r+} are produced in peripheral collisions with C_{60}.

As mentioned above, r-distribution associated with individual C_m^+ can be derived from 2D-map of TOF and n_e distribution as shown in Fig.2. Figure 5 shows the results measured for 0.5 MeV Si^+ and 6 MeV Si^{3+} impacts [11]. It should be pointed out that from r-distributions one can obtain information about the ionization energy E_{ion} which is the second part of the total energy deposition as $E_d = E_{int} + E_{ion}$. This was done by our model calculation [10] based on the statistical energy deposition (SED) model [12, 13]. With the aide of the r-hold ionization probability P_r [13], the r distribution Y_r is written as

$$Y_r = \int P_r(E_k) w(E_{ion}) dE_{ion} \tag{1}$$

with

$$w(E_{ion}) = \frac{1}{\sqrt{2\pi}\sigma} \exp\left(-\frac{(E_{ion} - E_c)^2}{2\sigma^2}\right) \tag{2}$$

where E_c the most probable ionization energy, σ the standard deviation and E_k the total kinetic

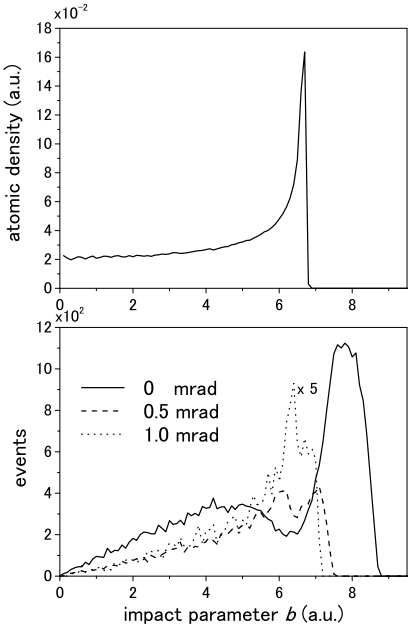

Figure 4. Calculated scattering yields at $\theta = 0, 0.5, 1.0$ mrad plotted as a function of the impact parameter b measured from the center of C_{60}.2MeV C+ on C_{60}. The upper shows number density of carbon atoms in C_{60}.

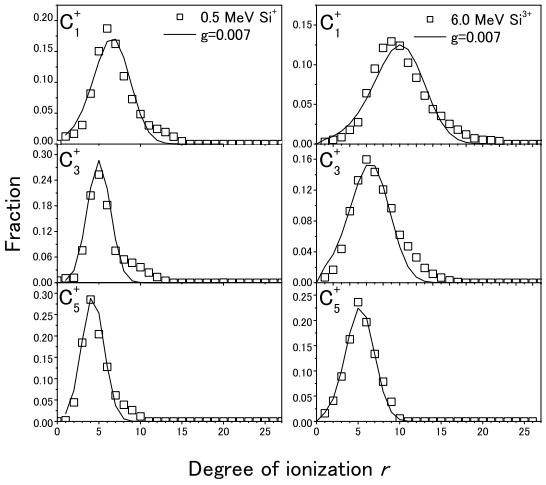

Figure 5. SED model calculations of r distributions correlated with C^+,C^{3+} and C^{5+}obtained for 0.5 MeV Si^+ and 6.0 MeV Si^{3+}single electron loss collisions with C_{60}.

energy of r ejected electrons with the relationship of

$$E_k(r) = E_{ion} - \sum_{i=1}^{r} I_i, \tag{3}$$

with I_i the i-th ionization potential of C_{60}. We applied Eq. (1) to our experimental r-distributions by treating σ and E_c as fitting parameters. Calculated curves are depicted by solid lines in Fig. 5, showing excellently good agreement with experimental distributions. The most probable ionization energies E_c obtained in this way for individual fragment ions are 820eV (C_1^+), 450eV (C_3^+) and 250eV (C_9^+) in case of 6MeV Si^{3+} impact. We stress that E_c can be deduced in our model calculation without knowledge of the kinetic energy carried away by secondary electrons. It is concluded that the SED model works fairly well to account for inelastic energy deposition in complicated collisions involving polyatomic molecules.

3.2. CO fragmentation

Apart from the target of C_{60}, diatomic and polyatomic molecules with line structure provide information about the orientation effect in molecular fragmentation. As a clear demonstration, we show in Fig.6 angular distributions of an ion pair (C^{2+}, O^+) produced from CO bombarded by 6 MeV O^{4+} ions. The data were taken for single electron capture and loss collisions associated with formation of $(CO)^{3+}$ as a predissociation parent ion. Here, the abscissa θ represents the molecular orientation angle between the beam axis and the CO molecular axis. It is well known

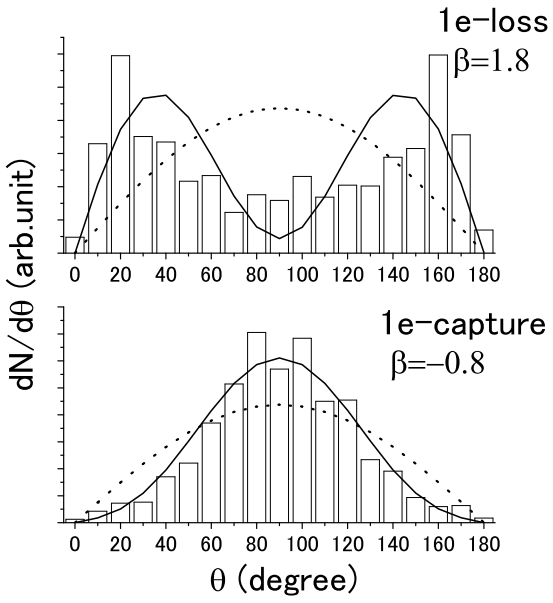

Figure 6. Production cross sections of the ion pair (C^{2+}, O^{+}) as a function of the molecular orientation angle θ measured for 1e-loss (upper) and 1e-capture (lower) collisions. Solid lines are the fitting results with Eq. (3) using anisotropy parameters β as denoted. Dashed lines show $\sin\theta$ for isotropic distributions.6MeV O^{4+} in CO

that the angular distribution in a diatomic molecule is described by the following formula [14]

$$N(\theta) \sim (1 + \beta P_2(\cos\theta)) \sin\theta \tag{4}$$

where $P_2(x) = (3x^2 - 1)/2$ and β is the anisotropy parameter. The experimental distributions were fitted to this equation and the results are shown by solid lines. Note that isotropic fragmentation (β =0) is drawn by a dashed line as a reference. Fitting results are reasonably in good agreement with experimental curves. It is obvious that fragmentation associated with capture collisions seems more isotropic while it is highly anisotropic in loss collisions. On the other hand the fragmentation from $(CO)^{2+}$ into (C^{+}, O^{+}) was found to be isotropic in both loss and capture collisions. This implies that the triple ionization of CO occurs preferentially in parallel collisions ($\theta \simeq 0, 180^{\circ}$) compared to perpendicular collisions. These features can be safely explained as follows. Ionization (electron loss) of O^{4+} with the ionization potential of 114 eV by a neutral CO is restricted to small impact-parameter collisions because a large inelastic energy is required to remove a tightly bound projectile electron. In parallel collisions, a projectile ion can undergo close collisions two times with C and O atoms and increases the electron loss probability compared to perpendicular collisions. By contrast, electron capture by O^{4+} can occur in distant collisions. Obviously the distant collision does not depend greatly on the orientation angle, resulting in isotropic distribution. It is noteworthy to refer to experimental results of Siegmann *et al* obtained for diatomic molecules [14, 15]. In their experiments, however, fragment ion pairs were measured without coincidence with projectile final charge states. They showed that fragmentation from $(CO)^{r+}$ or $(N_2)^{r+}$ becomes anisotropic with increasing r due to close collisions. These results are qualitatively consistent with our results.

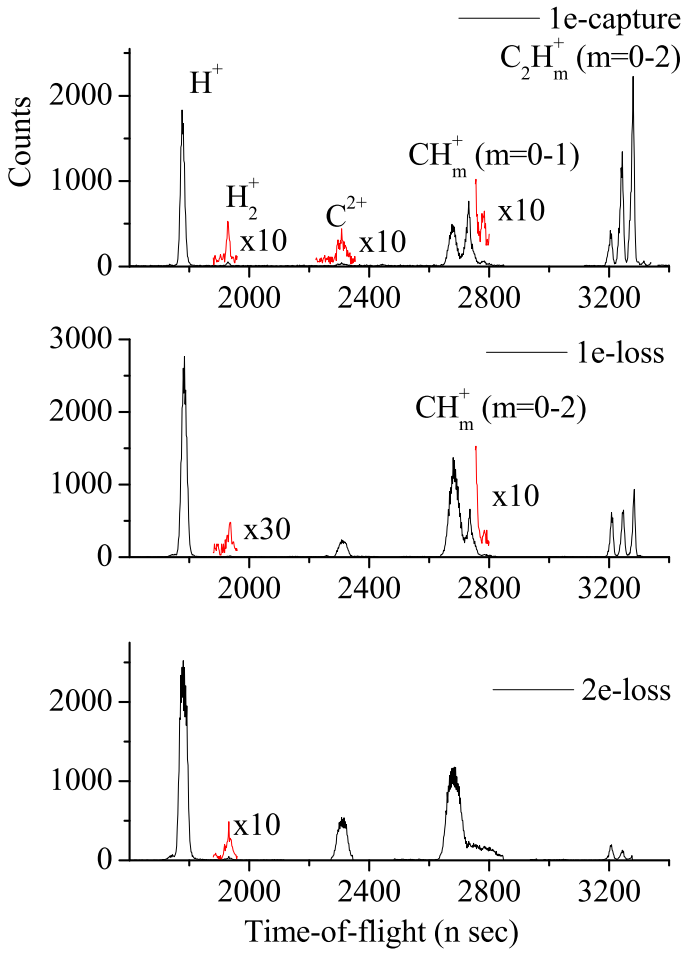

Figure 7. (Color online) TOF spectra in collisions between 2MeV Si^{2+} and C_2H_2

3.3. C_2H_2 fragmentation

Collision induced fragmentation of polyatomic molecular targets opens several new relaxation channels such as emission of fragment molecular ions, bond rearrangement or structure deformation. As for acetylene, there are some experimental investigations using photon impacts [16, 17]. In this work, we investigated acetylene fragmentation in charge changing collisions of 2 MeV Si^{2+} ions. TOF spectra measured in these collisions are shown in Fig. 7. Predominant products are H^+, C^{r+} (r =1,2), CH^+, C_2^+ and $C_2H_m^+$ (m =1,2). In addition, molecular ions formed through bond rearrangement dynamics are also observed weakly; see the peaks of H_2^+ and CH_2^+. It is interesting to point out that the doubly charged parent ion $(C_2H_2)^{2+}$ is not observed in our collision condition, while this peak was observed rather strongly in 1.2 MeV Ar^{8+} collisions [18]. It suggests that, in our lowly charged ion impact, $(C_2H_2)^{2+}$ is formed to unstable electronic or vibrational excited states, resulting in fragmentation. Close inspection of these spectra reveals rather large different profiles depending on the type of charge changing. Namely, the dominant products are $C_2H_m^+$ in single electron capture, while those in two-electron loss collisions are CH_m^+ produced via bond-breaking reactions. This fact reflects different impact parameters effective in capture and loss collisions.

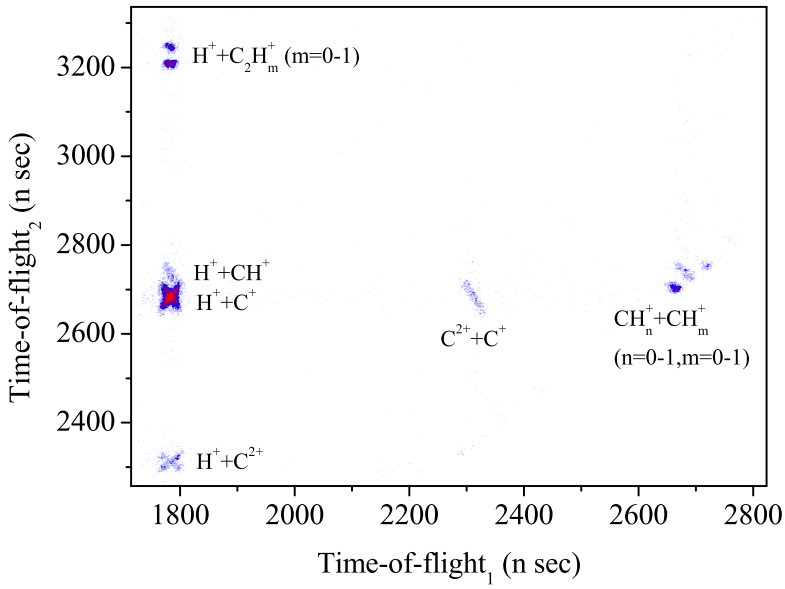

Figure 8. (Color online) TOF 2D spectra of fragment ions obtained in collisions between 2MeV Si^{2+} and C_2H_2

Figure 8 shows two-dimensional correlation map between two fragment ions produced in single collision events measured for 1e-loss collisions of 2MeV Si^{2+} ions. By analyzing 3D momentum data of these fragment ions we obtained kinetic energy release (KER) in various fragmentation channels from acetylene. Figures 9 and 10 present KER spectra in fragmentation channels of $C_2H_2 \longrightarrow (C_2H^+,H^+)$ and (C^+,C^+), respectively. Two peaks at about 3eV and 5 eV in (C_2H^+,H^+) may be assigned as the following fragmentation process [16],

$$Si^{2+} + C_2H_2 \rightarrow \quad C_2H_2^{2+*}(^1\Sigma_g^+) \rightarrow C_2H^+(^3\Pi) + H^+ \quad (\mathrm{KER} = 3\mathrm{eV}) \tag{5}$$

$$Si^{2+} + C_2H_2 \rightarrow C_2H_2^{2+*}(^1\Pi_u^+) \rightarrow C_2H^+(^1\Delta \text{ or } ^1\Sigma) + H^+ \quad (\mathrm{KER} = 5\mathrm{eV}) \tag{6}$$

Compared to Fig. 9 the KER spectra in (C^+,C^+) channel are broad and tailing to higher energies and are different considerably from capture to loss collisions. The results indicate that the (C^+, C^+) channel is attained through many intermediate dissociation channels. If the coulomb explosion model is applied to this channel, the KER estimated from $14.4/R$ between two C^+ ions is about 12 eV with $R = 1.21$Åthe interatomic distance between two carbon atoms. Hence, the binary explosion model is ruled out.

4. Summary

In summary, we described briefly our recent experimental data concerning molecular fragmentation of CO, C_2H_2 and C_{60} induced in charge changing collisions of fast heavy ions. It was found that the statistical energy deposition model works fairly well to reproduce experimental charge-state distributions of prefragmented C_{60}^{r+}. In particular, the ionization energy E_{ion} imparted to a molecule can be derived in our model calculations. It is pointed out

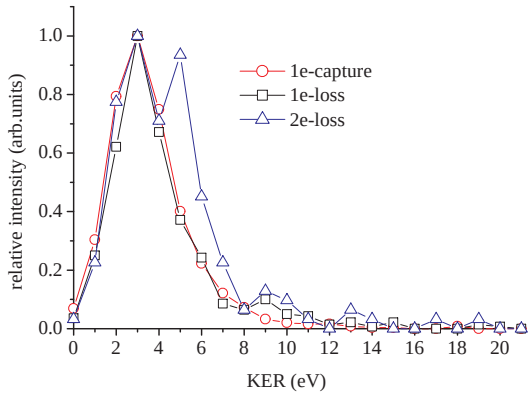

Figure 9. (Color online) KER spectra in a fragmentation channel (C_2H^+,H^+) obtained for 2MeV Si^{2+} collisions with C_2H_2.

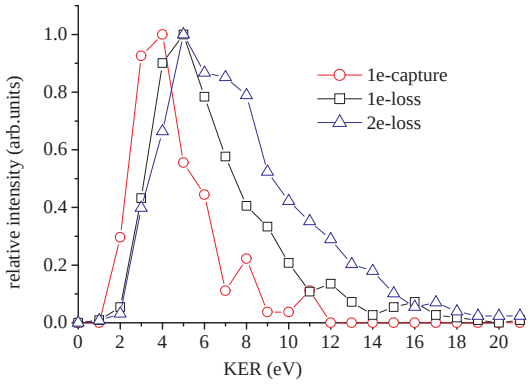

Figure 10. (Color online) The same as in Fig. 8 but for a fragmentation channel (C^+,C^+) .

that, once the amount of E_{ion} is known, the total energy deposition E_d into a target molecule may be deduced.

In collisions with CO and C_2H_2, molecular fragmentation was investigated in relationship with molecular orientation with respect to the incident ion beam, The kinetic energy distribution of fragment ions provides information about transient molecular excited states. To obtain further systematic information about molecular fragmentation, a series of hydrocarbons are investigated in our laboratory.

The work supported by Quantum Science and Engineering Center of Kyoto University.

* Present address: RIKEN (The Institute of Physical and Chemical Research), Wako 351-0198, Japan

Reference

[1] E. E. B. Campbell and E. Rohmund, 2000 *Rep. Prog. Phys.* **63** 1061
[2] J. Ullrich, *et. al.*, 2003*Rep. Prog. Phys.* **66** 1463
[3] T. Kaneyasu, T. Azuma, K. Okuno, 2005 *J. Phys. B: At. Mol. Opt. Phys.* **38** 1341
[4] A. Itoh, H. Tsuchida, T. Majima, and N. Imanishi, 1999 *Phys. Rev. A* **59** 4428
[5] B.L.S Brondsted *et al.*, 2006 *Phys. Rev. Lett.* **97** 133401(2006)
[6] T. Majima, Y. Nakai, T. Mizuno, H. Tsuchida, and A. Itoh, 2006 *Phys. Rev. A* **74** 033201
[7] T. Mizuno, T. Yamada, H. Tsuchida, Y. Nakai, and A. Itoh, 2010 *Phys. Rev. A* **81** 012704
[8] S. Sobottka and M. Williams, 1988 *IEEE Trans. Nucl. Sci.* **35** 348
[9] T. Majima, Y. Nakai, H. Tsuchida and A. Itoh, 2004 *Phys. Rev. A.* **69** 031202.
[10] T. Mizuno, D. Okamoto, T. Majima, Y. Nakai, H. Tsuchida and A. Itoh, 2007 *Phys. Rev. A* **75** 063203
[11] T. Mizuno, H. Tsuchida, T. Majima, Y. Nakai, and A. Itoh, 2008 *Phys. Rev. A* **78** 053202
[12] N. M. Kabachinik, V. N, Kondratyev, Z. Roller-Lutz, and H. O. Lutz, 1997 *Phys. Rev. A* **56** 2848. *ibid.*, 1998 **57** 990
[13] A. Russek, and J. Meli, 1970 *Physica* **46** 222
[14] B. Siegmann et al. 2002 *Phys. Rev. A.* **66** 052701
[15] B. Siegmann, U. Werner, H. Lebius, B. Huber, H. O. Lutz, R. Mann, 2003 *Nucl. Instr. and Meth. B* **205** 629
[16] T. Osipov T *et.al.* 2003 *Phys. Rev. Lett.* **90** 233002
[17] A. Hishikawa, A. Matsuda, M. Fushitani and E. Takahashi, 2007 *Phys. Rev. Lett.* **99** 258302
[18] S. De, J. Rajput, A. Roy, P.N. Ghosh and C. P. Safvan, 2008 *Phys. Rev.A.* **77** 022708